Hybrid crankshaft control for the reduction of torsional vibrations and rotational irregularities

Guillaume PAILLOT[1], Simon CHESNÉ[1], Didier RÉMOND[1]

[1]Univ Lyon, INSA-Lyon, CNRS UMR5259, LaMCoS, F-69621, France
guillaume.paillot@insa-lyon.fr

Abstract

Rotative systems do not have a constant revolution speed. The problem is even more significant in internal combustion engines, where the crankshaft is submitted to a torque that is far from being constant over a revolution period. This matter causes unacceptable noises in the the gearbox and fatigues the shaft, and it can be even further amplified by the shaft dynamics. This well-known problem is already tackled by numerous passive systems, and some active devices are being introduced to further enhance their capabilities. However, these ones are complex, not always fail-safe, need a control unit and consume high levels of energy.
In this paper, the authors introduce a hybrid self-fed damper for the so-called rotational irregularities, based on a tuned massed damper controled through an electromagnetic coupling by the irregular behaviour itself. For a better description, the whole behaviour of this non-stationary process is governed with an angular approach.

1 Introduction

In an internal combustion engine, the impulse initiated by the combustion of gas within the cylinders is able to put the crankshaft into a rotating movement, thus transmitting a torque to the wheels through the drivetrain. However, the movement of the piston is not uniform, and the transmitted torque is far from being constant at a steady engine regime [1]. Indeed, the important pressure variations on the piston as well as the influence of the alternating mass inertia create a periodic oscillation around an average value in torque. This creates a similar oscillation in angular acceleration, speed, and position, which is commonly referred to as rotational irregularities.
This oscillation tends to generate unacceptable noises, such as rattling noise in the gearbox, and fatigues the drivetrain parts, shortening the operating lifetime. For these reasons, such irregularities need to be reduced, which is traditionally done by a flywheel located between the crankshaft and the gearbox, while a viscous Lanchester damper on the front end reduces the torsional magnitude through energy dissipation. However, due to the downsizing of engines for fuel-consumption reasons, the simple flywheel is not enough anymore for acceptable noise levels.
This rotational irregularity phenomenon can be further amplified when the critical frequency of the crankshaft is a multiple of the current engine average speed. Here again, downsizing is a problem as a crankshaft length reduction increases the critical frequency, enabling a larger spectrum of engine speeds to excite the resonance. The presence of the viscous damper ensures that the crankshaft does not immediately break, but at the cost of a dissipated power up to 1kW for heavy duty vehicles.

For those reasons, there is a continuous research for more efficient solutions tackling the two presented issues : mitigation of the torsional levels in service and especially at the critical frequencies, and reduction of the dissipated energy in the damper. A large amount of passive solutions have been introduced over the two last decades in order to decrease the magnitude of torsional motions, typical examples being the Double (or Triple) Mass Flywheel ([2],[3]), variable inertia flywheels ([4],[5]), planetary gear systems ([6]), or Centrifugal Pendulum Vibrations Absorbers ([7],[8],[9]). These latter rely on the creation of an extra degree of freedom, enabling an "escape way" during resonance. However, its behaviour is still dependent on the steady engine regime, complicating a tuning process[10].

Some active concepts have also been proposed ([11],[12],[13],[14]), as the control possibilities they offer greatly enhance the capabilities of such dampers. Their limitation is the need for a power source.
Regarding the second issue, a promising way would be to collect the otherwise dissipated energy, and to store it so that it can be used by other devices in the vehicle. Several possibilities exist for the conversion, based on piezoelectricity - R-EHVTA [15] or pendulum harvester [16] - or on electromagnetic coupling, with some concepts developped over the last years, such as [17] or [18].

In this paper, the authors introduce a concept for a new self-fed rotational hybrid damper, combining an electromagnetic harvester with a hybrid Tuned Mass Damper (hTMD), that has already proved its capabilities for translational motions applications [19]. It is based on the generation of a counteracting torque by a set of permanent magnets and coils, similar to what happens in active dampers, coupled with the principle of the TMD, efficient against resonance issues. The TMD embeds a permanent magnet that moves in a coil. Both movements will change the local magnetic fields and generate an induced current in a common circuit, acting on each other.
In order to tackle non-stationary operating conditions, the present model involves angular and time approaches to describe the cyclic excitations and the frequency resonances.

2 Model building, important concepts and assumptions

The present concept can be applied to any rotating shaft submitted to rotational irregularities, no matter their profile. However in this paper we consider a 6-cylinder crankshaft, each with a cubic capacity of 1,3L.

2.1 Mechanical model

The crankshaft is first reduced to a 2 DoF-in-torsion part, as only the first torsional mode is of interest in this academic first application. As described in Fig.1, a regime-dependant cyclic excitation C_{exc} is introduced on the front degree of freedom. This excitation is the sum of the the torque produced by the explosion in the cylinders and of inertial effects. It is further described in the next section.
The measures are conducted on both ends, the second being the output of the shaft, connected to the gearbox. On this one, a resistive torque C_c assumed constant is applied, so as to balance the system and enable a steady speed. The actual interest is indeed the difference between both angles $\theta_2 - \theta_1$ for a constant engine regime. Numerical values of the introduced parameters are to be found in Table.1.

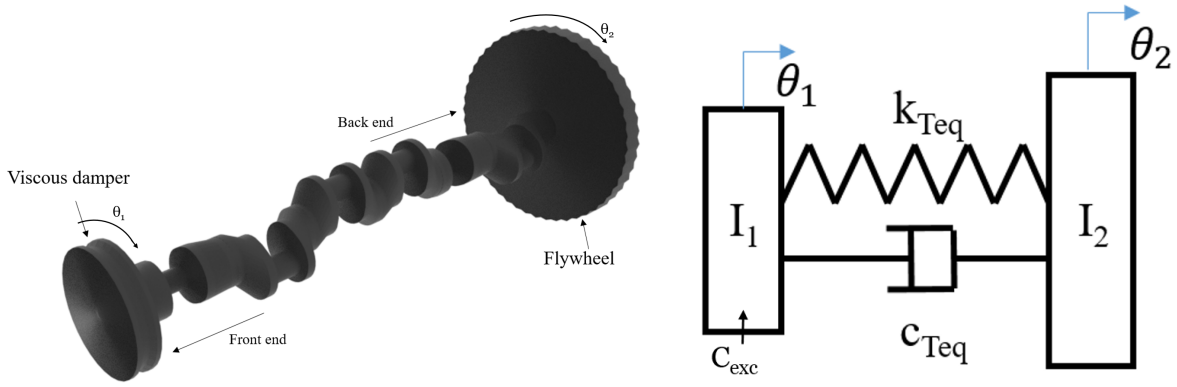

(a) Full crankshaft (b) Reduced model

Figure 1 – Model reduction

This model is governed by the system of equations :

$$\begin{cases} I_1\ddot{\theta}_1 + c_{Teq}(\dot{\theta}_1 - \dot{\theta}_2) + k_{Teq}(\theta_1 - \theta_2) = C_{exc} \\ I_2\ddot{\theta}_2 + c_{Teq}(\dot{\theta}_2 - \dot{\theta}_1) + k_{Teq}(\theta_2 - \theta_1) = -C_c \end{cases} \tag{1}$$

Parameter	Value
I_1	0.23 kg.m^2
I_2	1.65 kg.m^2
k_{Teq}	524 114 Nm/rad
c_{Teq}	100 Nms/rad

Table 1 – Parameters of the 2-DoF model

In a perfect engine, the natural frequency is excited only by the orders that are multiples of the number of cylinders, N_{cyl}, devided by two. To that extent, only the orders multiple of 3 are here taken into account. According to Table 2, as our engine speed range is from 600RPM to 2600RPM and the natural frequency is 256,8 Hz, we can restrict the analysis up to the 24th order : higher orders will not excite the natural frequency .

Order	Engine steady regime
3	-
6	2569 RPM
9	1713 RPM
12	1285 RPM
15	1028 RPM
18	857 RPM
21	734 RPM
24	642 RPM

Table 2 – The investigated orders and the corresponding engine regime at resonance

2.2 Excitation torque profile and non-stationary conditions

In a 4-stroke internal combustion engine, a complete period is accomplished in two revolutions, each stroke corresponding to half a revolution. Among them, only the firing stroke produces a useful torque, with a non-constant force over the revolution. However, the presence of the crank also causes it to be highly dependant on the instantaneous position α, as it is depicted in Fig.2. Noting λ the ratio of the rod length L_B to the crank radius R, F_{bg} the projection on the rod of the gas-induced force and d its lever arm, a geometric projection of $C_g = -F_{bg}.d$ brings :

$$C_g(\alpha) = -F_g(\alpha) \cdot R \cdot \sin(\alpha) \cdot \left(1 + \frac{\cos(\alpha)}{\sqrt{\lambda^2 - \sin(\alpha)^2}}\right) \tag{2}$$

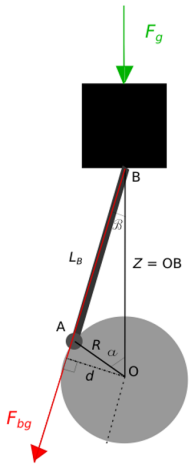

Figure 2 – Crankshaft, piston and rod

The force F_g, created by the explosion in the piston, is also dependant on the engine steady regime. In this expression, a constant part is the engine torque, and the oscillations around it are a first source of rotational irregularities.

The second source originates from the motions of the masses around and above the axis : the sum of the forces created by their inertias is not 0. Here again, there is a strong dependence on the instantaneous angular position, and also on the instantaneous angular speed. We note m_{alt} the mass considered in a translational motion when the shaft rotates. Assumed that the inertias do not change with speed and position :

$$\begin{cases} F_i = -m_{alt}.\dfrac{d^2Z}{dt^2} \\ Z = R\Big(\cos(\alpha) + \sqrt{\lambda^2 - \sin(\alpha)^2}\Big) \\ C_i = -F_i.R.\Big(cos(\alpha) + \sqrt{\lambda^2 - sin(\alpha)^2}\Big)\dfrac{sin\alpha}{\sqrt{\lambda^2 - sin(\alpha)^2}} \end{cases} \tag{3}$$

Which provides :

$$C_i = -m_{alt}.R^2\left(\left(sin(\alpha) + \frac{sin(2\alpha)}{2\sqrt{\lambda^2 - sin(\alpha)^2}}\right)\ddot{\alpha} + \left(cos(\alpha) + \frac{\lambda^2 cos(2\alpha) + sin(\alpha)^4}{(\lambda^2 - sin(\alpha)^2)^{3/2}}\right)\dot{\alpha}^2\right)sin(\alpha)\left(1 + \frac{cos(\alpha)}{\sqrt{\lambda^2 - sin(\alpha)^2}}\right) \tag{4}$$

The final excitation torque C_{exc} is the sum of the inertial torque and the oscillating gas torque. Its process is non-stationnary, though the simplifying stationary assumption $\alpha = \omega.t$ with a constant ω is often made. However, the instantaneous speed does not remain constant, since the input torque itself is harmonic : the angular acceleration is not 0, and its magnitude is directly linked to C_{exc}. In order to prevent any hidden behaviour to disappear in the analysis, and as the angular position θ_1 appears as the natural variable for such a rotating system, we use this variable instead of time for the resolution. The counterpart here is the introduction in the equations of a non-linear behaviour when the variable is swapped, as there is now a division by the instantaneous angular speed : $\frac{dX}{d\theta_1} = \frac{1}{\dot{\theta}_1}\frac{dX}{dt}$.

2.3 TMD model

First addition to the previous 2-DoF model is the mass damper, tuned on its resonance frequency according to Den Hartog's principles [20]. It consists in a magnet clamped on a mass, linked to the rotating shaft with a spring set at a certain distance R_{TMD} of the rotation axis. The resulting torsional stiffness k_{TMD} depends on the tuning. Around this magnet, a coil is set, clamped to the shaft, in such a way that the TMD can translate within.

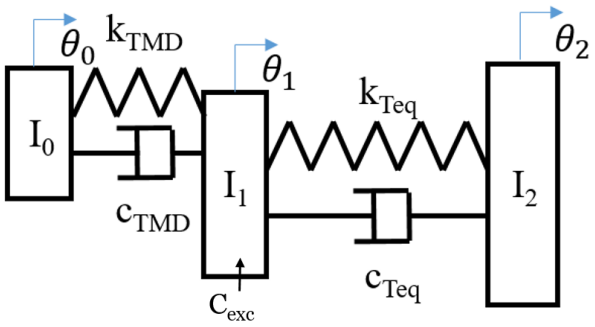

Figure 3 – Reduced model of crankshaft including a TMD in front position

However, as we want to control the torsional behaviour, determined by the difference of the angles, both degrees of freedom are potential candidates to host the TMD set, but the two will not act the same.
The front end has the greatest amplitude during vibration due to its lower inertia, and the lower the inertia, the lower the efficient modal inertia I_{eq}. At a given R_{TMD}, a lower mass for the TMD is then required, as the ratio of its inertia I_0 to I_{eq} is the key parameter of the tuning. To that extent, better performance can be achieved for

Parameter	Value
I_0	0.013 kg.m^2
μ	0.05
k_{TMD}	29 617 Nm/rad
c_{TMD}	7.36 Nms/rad
R_{TMD}	0.2 m
m_{TMD}	0.325 kg

Table 3 – Parameters of the 3-DoF model

a TMD on the front end and in the rest of the paper, this integration possibility is chosen, described in Fig.3. Its absolute angle around the rotation axis is parameterized by θ_0.
To bring what happens to the TMD in a more practical frame, let us define a relative variable for the new degree of freedom : $x = R_{TMD}(\theta_0 - \theta_1)$. This variable translates the torsional motion of the TMD around the axis of rotation in regard to the disc to which it is clamped. The values for all introduced parameters can be found in Table 3. The inertia ratio μ is chosen to 0.05, as this value allows a realistic mass and a realistic distance to the shaft to be chosen.

2.4 Electromagnetic model

The electromagnetic model actually consists in two parts. One has already been introduced in subsection 2.3, and describes the interaction of the magnet on the TMD and its surrounding coil. Indeed, any motion of the TMD creates an induced current in the coil, and conversely, any current circulating in the coil creates a magnetic field interacting with the magnet.

The second part is located around the flywheel. It consists in a set of coils and another of magnets, one being embedded in the flywheel and rotating with the shaft, the other being fixed in the vehicle, all around the flywheel. Again, moving a magnet close to a coil will create a current, itself generating a magnetic field that will slow down the motion, according to Lenz's law, and eventually damp the rotational irregularities. We note ϕ the magnetic flux.

The red arrows in Fig.4a show the different electromagnetic interactions that occur. The two parts are linked to another through an impedance Z_{EM}, as to be seen in Fig.4b. What this impedance covers depends on the interaction scenario.

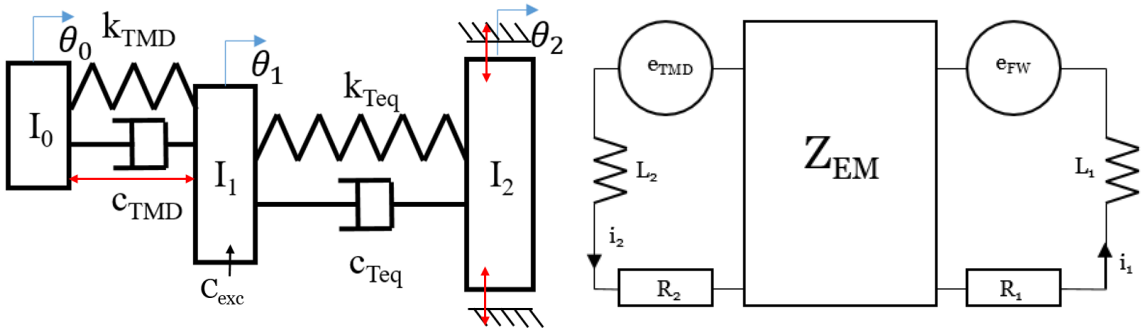

(a) Reduced model with EM interactions

(b) Electromagnetic circuit

Figure 4 – Electromagnetic model

With the electromotive forces e_{FW} at the flywheel and e_{TMD} at the TMD, defined as:

$$\begin{cases} e_{FW} = -\dfrac{d\phi}{dt} \\ e_{TMD} = -T_2\dot{x} \end{cases} \tag{5}$$

and under the assumption that $Z_{EM} = 0$, the total model can thus be described with a system of five equations, three mechanical equations and two electrical ones :

$$\begin{cases} I_0\ddot{x} + (1+\frac{I_0}{I_1})(c_{TMD}\dot{x} + k_{TMD}x) - \frac{I_0}{I_1}R_{TMD}(c_{Teq}(\dot{\theta}_1 - \dot{\theta}_2) + k_{Teq}(\theta_1 - \theta_2)) = -\frac{I_0}{I_1}R_{TMD}.C_{exc} + R_{TMD}^2 T_2 i_2 (1+\frac{I_0}{I_1}) \\ I_1\ddot{\theta}_1 + c_{Teq}(\dot{\theta}_1 - \dot{\theta}_2) + k_{Teq}(\theta_1 - \theta_2) - \frac{c_{TMD}}{R_{TMD}}\dot{x} - \frac{k_{TMD}}{R_{TMD}}x = C_{exc} - R_{TMD}^2 T_2 i_2 \\ I_2\ddot{\theta}_2 + c_{Teq}(\dot{\theta}_2 - \dot{\theta}_1) + k_{Teq}(\theta_2 - \theta_1) = -C_c + T_1.R_{ext} i_1 \\ L_1\frac{di_1}{dt} + R_1 i_1 = -pT_1\dot{\theta}_2 \\ L_2\frac{di_2}{dt} + R_2 i_2 = -T_2\dot{x} \end{cases} \tag{6}$$

Where T_2 is the coupling factor depicting the electromagnetic interaction between the TMD and the surrounding coil [21], p is a scalar and T_1 is a coupling function linked to $\frac{d\phi}{dt}$. Both are further described in the next subsection.
In the case where the TMD is actually located on the flywheel, or depending on Z_{EM}, these equations can be slightly different.

2.5 The T_1 function and p parameter

In subsection 2.2, we have stated that an angular approach is better suited to describe the rotation of the shaft and the irregularities that occur. Moreover, Faraday's law states that the electromotive force is proportional to the time derivative of the magnetic flux, which itself is then a function of the instantaneous angular position, here measured at the flywheel. Changing the variable t to θ_2 provides $e_{FW} = -\dot{\theta}_2\frac{d\phi}{d\theta_2}$.
On the other hand, the countering torque C_{count} created at the flywheel by the current also depends on the location of the various coils and magnets. It is able to mitigate the rotational irregularities when it and the excitation torque C_{ext} have the same main harmonics, but with a 180° phase shift. Assuming this torque and $\frac{d\phi}{d\theta_2}$ have a same sine shape involving the same harmonics, the introduced T_1 function aims to bridge the gap between them. To that extent, the torque exerted when a number n of coils and a number m of magnets interact during the revolution can be described using the expression :

$$T_1 = \sum_{i=1}^{n}\sum_{j=1}^{m} K_{i,j} m_j \mu_0 \frac{N_i}{L_{sol,i}} sin(\beta_{i,j}) \tag{7}$$

and the relationship :

$$C_{count} = T_1.R_{ext} i_1 \tag{8}$$

In (7), N_i is the number of turns in solenoid i, $L_{sol,i}$ the length of the same solenoid, m_j the magnetic moment of magnet j, and K is a matrix describing the coupling coefficient between coil i and magnet j. $\beta_{i,j}$ is a local variable standing for the angular position θ_2 when a magnet interacts with a coil.
With this description, we also have the relationship :

$$e_{FW} = -p\dot{\theta}_2 T_1 \tag{9}$$

the description of the harmonics being included in T_1, except for their amplitude. To that extent, in order to keep realistic values for the electromotive force e_{FW}, we introduce an additional parameter, p, which purpose is to adjust the magnitude of the harmonics.

3 Model results

3.1 Efficiency of the TMD

To display the efficiency of the concept in our model, let us first consider a decoupled electromagnetic circuit, as modeled in Fig.5a. With a low value for T_2, the created current is very low, and the natural motion of the TMD is almost not impeded. Regarding the electromagnetic setup around the flywheel, there is also

little impact on the overall rotation as the countering torque C_{count} is four orders of magnitude lower than the excitation torque C_{exc}. Such configuration is equivalent to actually no circuit at all, and enables to measure the effect of a passive TMD.

As we can see on the Bode diagram in Fig.5b, the TMD flattens the peak at the natural frequency of the torsional mode. The tuning parameters used are those detailed in Table.3. This enables a reduction of 15% the amplitude in torsion, as displayed in Fig.6a for the response at 2600RPM. At this regime, the 6^{th} order excites a frequency which is very close to the natural frequency. At 2200RPM, situation displayed in Fig.6b, the frequencies excited are further from the natural frequency, and the damping is smaller, even though still present.

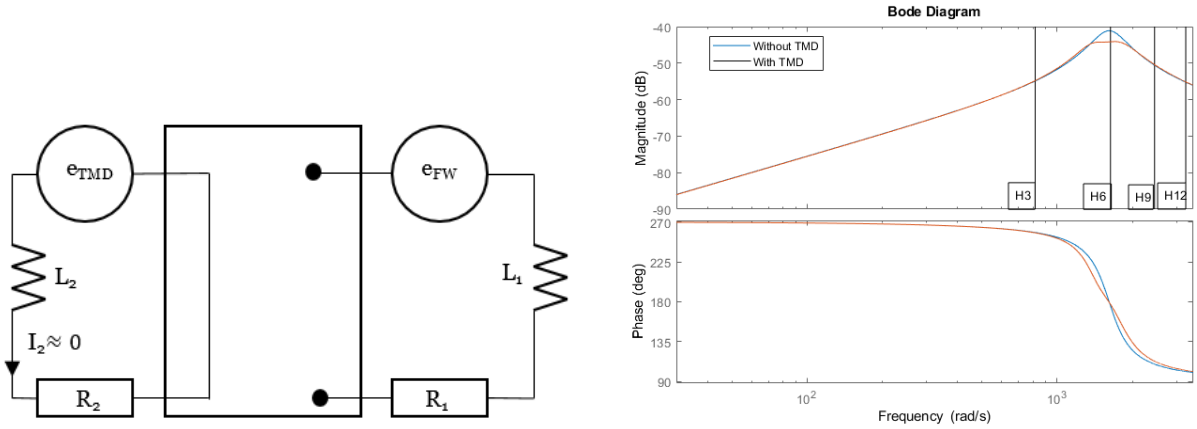

(a) Decoupled electromagnetic circuit

(b) Bode diagram with the harmonics at 2600RPM

Figure 5 – Passive TMD scenario

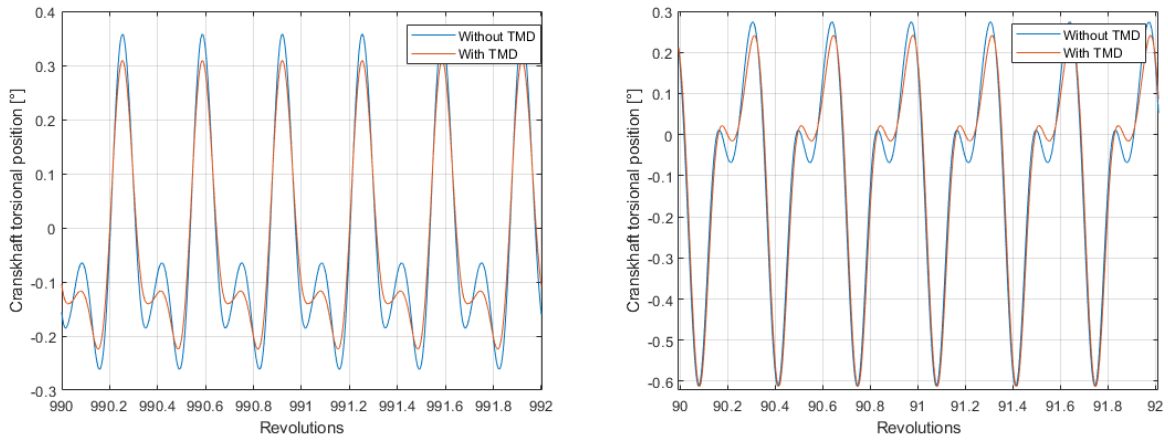

(a) At 2600RPM

(b) At 2200RPM

Figure 6 – Typical magnitude reductions

3.2 Coupling effect in the hybrid damper

Now let us consider a direct hookup between the two constituents of the electromagnetic circuit, a situation depicted in Fig.7. The equations in (6) must then be changed, as it is now imposed $i_1 = i_2$. The parameters used are listed in Table.4. In this situation, we still have $Z_{EM} = 0$

Parameter	Value
L_1	555mH
L_2	185mH
R_1	15.51Ω
R_2	5.17Ω
T_2	0.8
p	0.25
$T_1(\theta)$	$0.01.sin(6\theta)$

Table 4 – Parameters for the coupled model

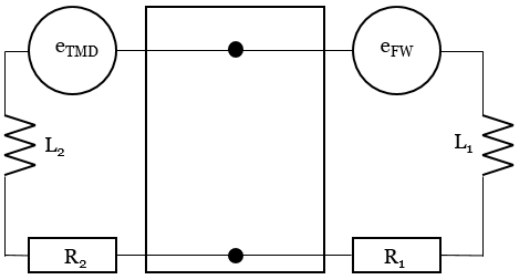

Figure 7 – Direct hookup electromagnetic circuit

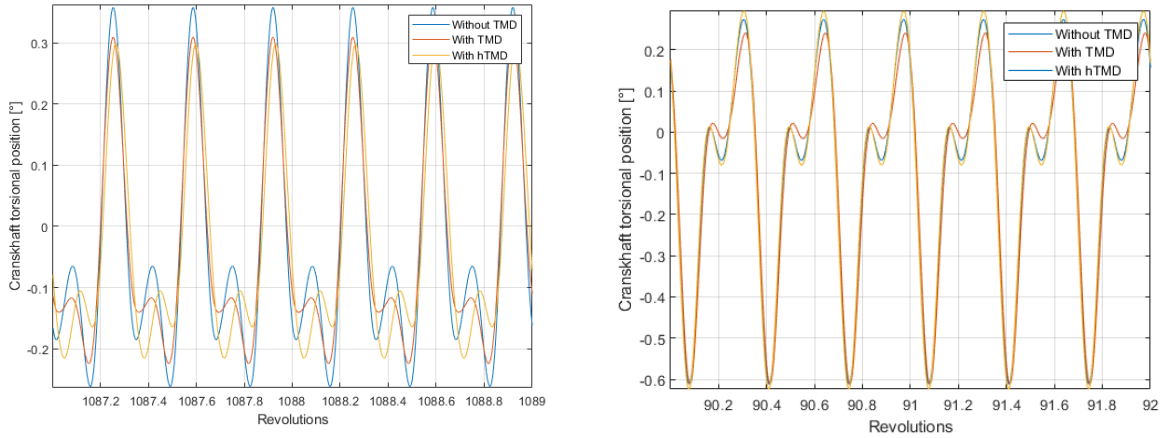

(a) At 2600 RPM

(b) At 2200 RPM

Figure 8 – Comparison with the previous case

As we can see in Fig.8a, at 2600RPM in that particular situation, the damping is slightly better, even though the values considered are not tremendous. However, this results must be handled carefully, since no phase effect has yet been taken into account in T_1, effects that could make the hTMD ineffective or even worsen the situation, which is what appears at 2200RPM in Fig.8b. Indeed, the hookup is equivalent to a modification of c_{TMD} and - to a lesser extent - of k_{TMD}. A modification of the damping factor can thus be advantageous or detrimental, and what happens is highly dependent on the involved harmonics and phases, and on the hookup configuration. To that extent, it appears necessary to further investigate on the effect of each harmonic's phase and on the configurations for Z_{EM}, in order to properly damp the torsional mode in all cases.

Discussion - Conclusions

In this paper, a new concept for a hybrid mass damper against rotational irregularities has been introduced and described. The self-fed property avoids any exterior source of power, but also complicates the tuning of the system due to the instantanous angular position and the steady regime dependence. The interaction between the two parts of the electromagnetic circuit is not yet fully understood, whereas this is a major requirement to have them work together properly. Indeed, it has been seen in 3.2 that a direct hookup can provide unexpected behaviour if the phases are not carefully handled.
Further work will also be devoted to a check of the assumptions that are made. In particular, it is necessary to prove the possibility to approximate the $\frac{d\phi}{d\theta_2}$ function to a sine with given harmonics. There is also no guarantee that any harmonic signal can be approximated by at least one particular coil-and-magnet spatial layout. The tayloring is quite straightforward when only one or two harmonics are involved, though here 8 different harmonics are being investigated. However a truncation to the fundamental or to a predominant harmonic could be sufficient to efficiently damp the rotational irregularities. In all cases, further work on the damping possibilities of such a hTMD is expected, in order to present its capabilities in comparison to a fully passive TMD.
The hookup of the full electromagnetic circuit in a real engine also matters. It has been stated in 2.3 that the TMD is more efficient when mounted on the lower inertia, however the rest of the electromagnetic circuit is necessarily mounted on the flywheel, which is the other end of the crankshaft. In this configuration, it is nessary to embody the wires along the shaft in the rotating referential. The choice is left to equip the flywheel with the TMD instead, in another configuration that provides a better integration rate at the cost of a lower performance.

Acknowledgements

This work has been supported by the chair 'Solutions for the future of Road Freight Transport', jointly created by INSA Lyon LaMCoS and Volvo Group.

References

[1] J.-L. Ligier and E. Baron, *Acyclisme et vibrations: applications aux moteurs thermiques et aux transmissions. 1, Notions de base*. Paris, France: Ed. Technip, 2002, ISBN: 978-2-7108-0820-6.

[2] U. Schaper, O. Sawodny, T. Mahl, and U. Blessing, "Modeling and torque estimation of an automotive dual mass flywheel", in *2009 American Control Conference*, St. Louis, MO, USA: IEEE, 2009, pp. 1207–1212, ISBN: 978-1-4244-4523-3. DOI: 10.1109/ACC.2009.5160136.

[3] L. Wramner, V. Berbyuk, and H. Johansson, "Vibration dynamics in non-linear dual mass flywheels for heavy-duty trucks", in *Proceedings of ISMA2018 International Conference on Noise and Vibration Engineering*, 2018, pp. 1935–1947.

[4] X. Dong, "Magneto-rheological variable inertia flywheel", *Smart Materials and Structures*, vol. 27, no. 11, Jul. 2018.

[5] L. L. Schumacher, "Controllable inertia flywheel", U.S. Patent 4995282A, Feb. 26, 1991.

[6] A. Suryanarayana, "Engine dynamics and torsion vibration reduction", Master Thesis, Chalmers, 2015, 52 pp.

[7] D. E. Newland, "Developments in the design of centrifugal pendulum vibration absorbers", presented at the ICSV 24, 2017, p. 8.

[8] A. Kooy, Ed., *Isolation is the key*, Solving the Powertrain Puzzle: 10th Schaeffler Symposium April 3/4, 2014, Springer Vieweg, 2014, ISBN: 978-3-658-06194-4.

[9] M. Pfabe and C. Woernle, "Reduction of periodic torsional vibration using centrifugal pendulum vibration absorbers", *PAMM*, vol. 9, no. 1, pp. 285–286, 2009, ISSN: 1617-7061. DOI: 10.1002/pamm.200910116.

[10] K. Nishimura, T. Ikeda, and Y. Harata, "Localization phenomena in torsional rotating shaft systems with multiple centrifugal pendulum vibration absorbers", *Nonlinear Dynamics*, vol. 83, no. 3, pp. 1705–1726, Feb. 1, 2016, ISSN: 1573-269X. DOI: 10.1007/s11071-015-2441-2.

[11] J. Pfleghaar and B. Lohmann, "The electrical dual mass flywheel -an efficient active damping system", *IFAC Proceedings Volumes*, 7th IFAC Symposium on Advances in Automotive Control, vol. 46, no. 21, pp. 483–488, Jan. 1, 2013, ISSN: 1474-6670. DOI: 10.3182/20130904-4-JP-2042.00046.

[12] S. Schwunk, "Method for vibration damping of a drive train by means of an electric machine", U.S. Patent 20170334448A1, Nov. 23, 2017.

[13] A. Gruendl, B. Hoffmann, U. Masberg, T. Pels, and K.-P. Zeyen, "System zur aktiven dämpfung von drehungleichförmigkeiten der kurbelwelle eines verbrennungsmotors oder einer damit gekoppelten welle", European pat. 0847485B1, Jun. 23, 1999.

[14] F. Knopf and M. Steidl, "Verfahren zum aktiven isolieren eines antriebsstrangs von drehschwingungen einer welle einer maschine, insbesondere einer kurbelwelle einer hubkolbenmaschine, und eine entsprechende anordnung zur durchführung des verfahrens", pat. WO2014118246A1, Aug. 7, 2014.

[15] F. Infante, W. Kaal, S. Perfetto, and S. Herold, "Design development of rotational energy harvesting vibration absorber (r-EHTVA)", Sep. 10, 2018. DOI: 10.1115/SMASIS2018-7902.

[16] L. Gu and C. Livermore, "Pendulum-driven passive self-tuning energy harvester for rotating applications", *Applied Physics Letters*, p. 4,

[17] S. Troebst, "Dämpfungssystem mit Energierückgewinnung für ein Kraftfahrzeug und Antriebsvorrichtung mit einem derartigen Dämpfungssystem", European pat. 2910813A2, Aug. 26, 2015.

[18] B. Gunn, S. Theodossiades, and S. J. Rothberg, "A nonlinear concept of electromagnetic energy harvester for rotational applications", *Journal of Vibration and Acoustics*, Nov. 19, 2018, ISSN: 1048-9002. DOI: 10.1115/1.4042040.

[19] S. Chesne and C. Colette, "A simple hybridization of active and passive mass dampers", presented at the ISMA2016, KU Leuven, Sep. 2016.

[20] J. P. Den Hartog, *Mechanical vibrations*, 4th. New York, NY : McGraw-Hill, 1956, 446 pp.

[21] A. Preumont and B. Mokrani, *Electromagnetic and piezoelectric transducers*.